

HETEROCYCLES, Vol. 87, No. 1, 2013, pp. 31 - 54. © 2013 The Japan Institute of Heterocyclic Chemistry  
Received, 29th October, 2012, Accepted, 12th November, 2012, Published online, 16th November, 2012  
DOI: 10.3987/REV-12-757

## BORON AND PHOSPHORUS COMPLEXES OF MESO-ARYL EXPANDED PORPHYRINS

Tomohiro Higashino and Atsuhiko Osuka\*

Department of Chemistry, Graduate School of Science, Kyoto University, Sakyo-ku, Kyoto, 606-8502, Japan; E-mail: osuka@kuchem.kyoto-u.ac.jp

**Abstract** – Our recent efforts in the boron and phosphorus insertion reactions into *meso*-aryl expanded porphyrins are reviewed. Boron insertion into [28]hexaphyrin(1.1.1.1.1.1) **19** triggered a skeletal rearrangement to bis-boron complex of [28]hexaphyrin(2.1.1.0.1.1) **20**. Boron-insertion into quadruply *N*-fused heptaphyrin **23** with BBr<sub>3</sub> and EtN<sup>i</sup>Pr<sub>2</sub> followed by treatment with an alcohol gave corresponding boron complex **24-OR**. Treatment of non-fused heptaphyrin mono-Cu(II) complex **25** with BBr<sub>3</sub> and EtN<sup>i</sup>Pr<sub>2</sub> induced a splitting reaction to B(III) subporphyrin **26** and Cu(II) porphyrin **27**. Phosphorus insertion to *N*-fused [24]pentaphyrin **30** led to the formation of multiply fused P(V) complex **31**, which was reduced to P(III) complex **33** with BH<sub>3</sub>·Me<sub>2</sub>S as a rare P(III) porphyrinoid. Phosphorus insertion to **19** proceeded in a stepwise manner to give mono-P(V) complex **38** and bis-P(V) complex **39**, which were, respectively, identified to be Möbius aromatic and antiaromatic molecules. Phosphorus insertion into [34]heptaphyrin **40** gave Möbius antiaromatic P(V) complex **43** and Hückel aromatic P(V) complex **44**. Upon heating in acetonitrile, **43** was cleanly converted to **44**, indicating that **43** was a kinetically formed Möbius antiaromatic product as the first case. Phosphorus insertion into [36]octaphyrin **5** led to the formation of [38]octaphyrin mono-P(V) complex **47** and [40]octaphyrin bis-P(V) complex **48**. The latter complex is a fully reduced octaphyrin, hence representing the first example of expanded isophlorins, but is stable under ambient conditions.

## CONTENTS

1. Introduction
2. Boron and Phosphorus Complexes of Porphyrins
  - 2-1. Boron Complexes of Porphyrins

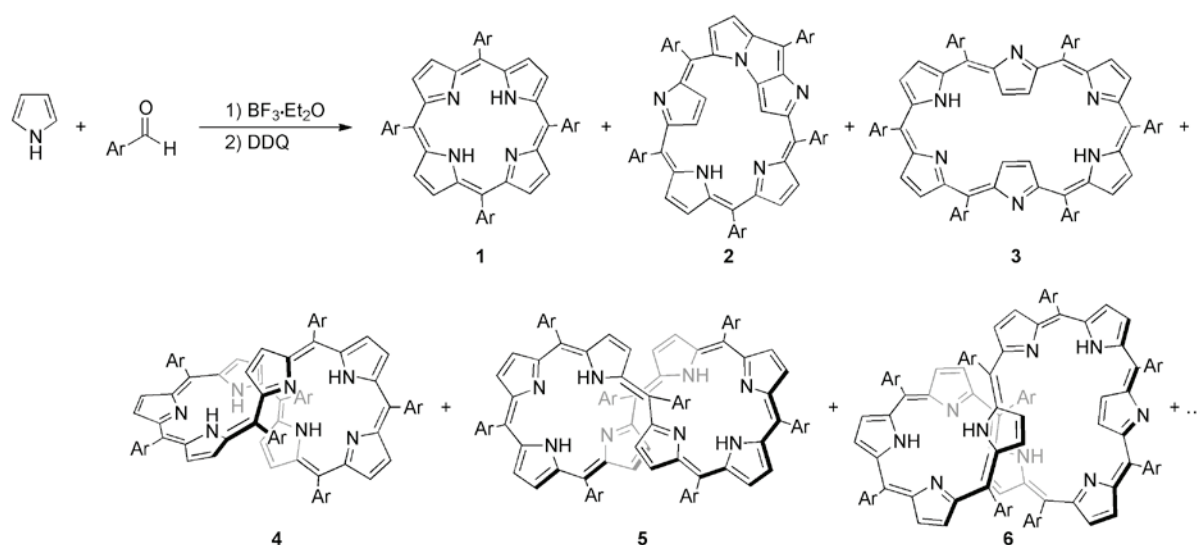
- 2-2. Phosphorus Complexes of Porphyrins
- 3. Boron Complexes of *meso*-Aryl Expanded Porphyrins
  - 3-1. Boron Insertion Induced Skeletal Rearrangement to Hexaphyrin(2.1.1.0.1.1)
  - 3-2. Boron Complexes of Heptaphyrin and Splitting Reaction
- 4. Phosphorus Complexes of *meso*-Aryl Expanded Porphyrins
  - 4-1. *N*-Fused Pentaphyrin (NFP<sub>5</sub>)
    - 4-1-1. General Properties
    - 4-1-2. Phosphorus Complexes of Triply Fused [24]Pentaphyrin
  - 4-2. Hexaphyrin
    - 4-2-1. General Properties
    - 4-2-2. Möbius Aromatic and Antiaromatic Phosphorus Complexes of Hexaphyrins
  - 4-3. Heptaphyrin
    - 4-3-1. General Properties
    - 4-3-2. Hückel Aromatic and Möbius Antiaromatic Phosphorus Complexes of Heptaphyrins
  - 4-4. Octaphyrin
    - 4-4-1. General Properties
    - 4-4-2. Phosphorus Complexes of Octaphyrin: Expanded Isophlorin
- 5. Conclusion

## 1. INTRODUCTION

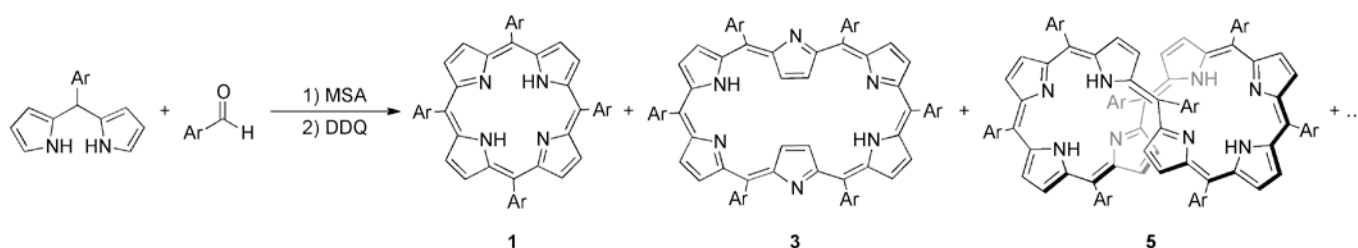
In recent years, there is a growing interest in the chemistry of expanded porphyrins that consist of more than five pyrrolic units.<sup>1</sup> Expanded porphyrins are homologues of porphyrins but possess attractive attributes such as multi-metal coordination capabilities,<sup>2</sup> versatile redox-states,<sup>3</sup> large nonlinear optical properties,<sup>4</sup> transannular bridging reactions,<sup>5</sup> metamorphosis-like mutual interconversions,<sup>6</sup> and effective platforms to realize stable Möbius aromatic and antiaromatic species,<sup>7</sup> which are not shared with porphyrins. We entered the chemistry of expanded porphyrins since our serendipitous finding of the effective synthesis of a series of *meso*-aryl substituted expanded porphyrins in the reaction of pentafluorobenzaldehyde and pyrrole.<sup>8</sup> In 1987, Lindsey *et al.* reported a simple two-step one-flask procedure for the synthesis of porphyrins that was based on the condensation of pyrrole and aromatic aldehyde at 6.7 mM using BF<sub>3</sub>·OEt<sub>2</sub> in CH<sub>2</sub>Cl<sub>2</sub>.<sup>9</sup> We found that when the condensation reaction of pyrrole and pentafluorobenzaldehyde was conducted at 10 times higher concentrations (ca. 67 mM), a series of *meso*-aryl expanded porphyrins were produced with acceptable yields.<sup>8</sup> This simple and effective synthesis is only applicable to 2,6-substituted electron-deficient aryl aldehydes. The size-selective synthesis of expanded porphyrins has been achieved by using dipyrromethane or tripyrrane as a building

block.<sup>10,11</sup> This size-selective protocol has advantages of better yields, easier separation, and availability of expanded porphyrins bearing two different *meso*-aryl substituents (Scheme 2).<sup>11</sup>

The systematic nomenclature of expanded porphyrins proposed by Franck and Nonn is employed in this account.<sup>12</sup> In this nomenclature, the name of expanded porphyrin consists of three parts: 1) the number in the bracket indicates the number of  $\pi$  electrons in the macrocyclic conjugation pathway, 2) the core name that indicates the number of pyrrole subunits, and 3) the numbers in the parentheses indicate the numbers of bridging carbon atoms between the constitutional pyrrole groups.



Scheme 1. One-pot synthesis of *meso*-aryl expanded porphyrins by a modified Rothmund-Lindsey method.



Scheme 2. Size-selective synthesis of *meso*-aryl expanded porphyrins.

The chemistry of main group porphyrin complexes has been actively studied. It is known that elements with the covalent radius ( $r_{\text{cov}}$ ) of 1.22–1.43 Å fit comfortably with a porphyrin cavity. Phosphorus and boron are considerably small ( $r_{\text{cov}} = 1.10$  and 0.85 Å, respectively), hence requiring structural distortion or doubly occupancy for their accommodation in porphyrin.<sup>13</sup> While various metal complexes of expanded porphyrins have been prepared so far,<sup>11,2</sup> their main group complexes have still remained rather limited. As rare examples, boron complexes of [22]hexaphyrin(1.0.0.1.0.0) (amethyrin) **7** and

[32]octaphyrin(1.0.0.0.1.0.0.0) **8** were reported as hydrolytically stable complexes by Sessler and co-workers in 2004 (Figure 1).<sup>14</sup> In this account, we summarized our recent advances in the chemistry of boron and phosphorus complexes of expanded porphyrins.

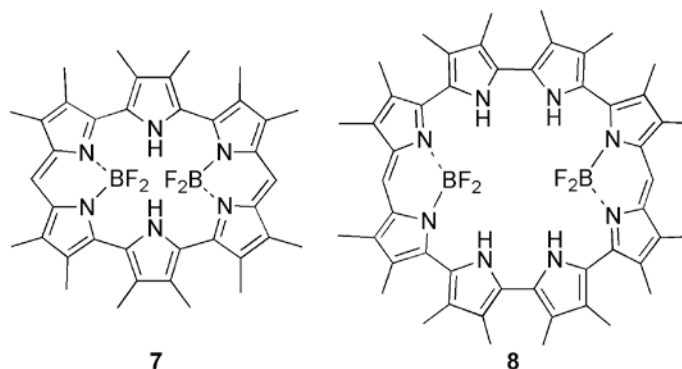


Figure 1. Boron complexes of expanded porphyrins.

## 2. BORON AND PHOSPHORUS COMPLEXES OF PORPHYRINS

### 2-1. Boron Complexes of Porphyrins

In 1970s, an attempt to prepare a boron complex of porphyrin was reported but the data were not sufficient for full characterization.<sup>15</sup> The first fully characterized boron complex **9** was reported by Brothers and co-workers in 1994,<sup>16</sup> which was accompanied by complex **10** in 1998.<sup>17</sup> They prepared these complexes by the reactions of TPP-type porphyrins with  $\text{BF}_3$  or  $\text{BCl}_3$  in the presence of a trace amount of water. They also reported that the reduction of dichlorodiboranyl complex **11** with magnesium anthracenide provided isophlorin complex **12**, which exhibited strong  $20\pi$  antiaromaticity.<sup>18</sup> In addition, Latos-Grażyński and co-workers prepared boron complex of *N*-fused porphyrin **13**, which represented a rare example of NNN-type, tripyrrolylboron complexes.<sup>19</sup>

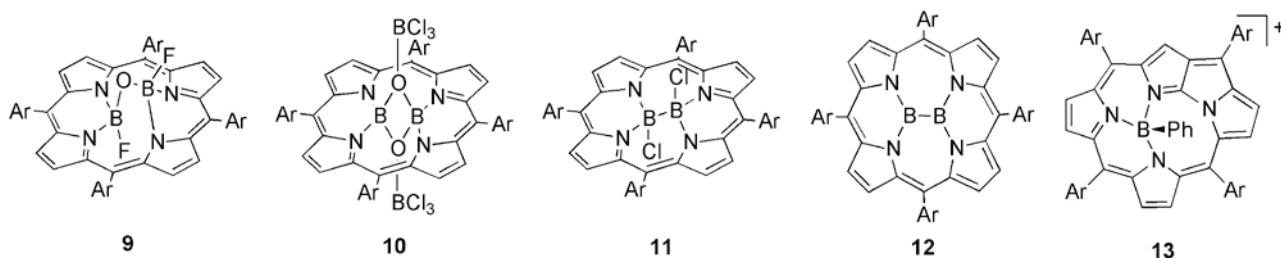


Figure 2. Representative examples of boron complexes of porphyrinoids.

### 2-2. Phosphorus Complexes of Porphyrins

Phosphorus is small for accommodation at the porphyrin core and hexa-coordination of the phosphorus(V) ion was proposed to result in a ruffled structure.<sup>20</sup> The first phosphorus complex was reported by Gouterman *et al.* in 1976.<sup>21</sup> Brothers synthesized a phosphorus(V) porphyrin **14** bearing

chloride anions as axial ligands, and she revealed that the chloro groups on phosphorus atom can be replaced by oxygen and nitrogen substituents.<sup>22</sup> Akiba *et al.* reported the synthesis of phosphorus porphyrin complexes that contained a phosphorus-carbon bond by reactions with organoaluminum reagents.<sup>23</sup> Phosphorus porphyrin complexes can be used as a structural motif to create oligomeric architectures. For example, the “wheel-and-axle”-type phosphorus(V) porphyrin arrays **15** were synthesized by Shimizu *et al.*<sup>24</sup> A porphyrin-based molecular electronic/optical device can be also constructed by utilizing the axial-bonding capability of phosphorus(V) porphyrin.<sup>25</sup>

Besides, phosphorus insertion has been recently shown to be also effective in creation of novel macrocycles. The rearrangement of tetraazaporphyrin into triazacorrole **16** was first reported by Hanack,<sup>26</sup> and Goldberg has widely used this method in the azacorrole chemistry.<sup>27</sup> Latos-Grażyński reported phosphorus complexes of *N*-fused porphyrin **17**<sup>28</sup> and *N*-fused telluraporphyrin **18**,<sup>29</sup> which are  $20\pi$  porphyrin, isophlorin analogues. It is notable that phosphorus atom was bound to NNN- or NNC-manner as the P=O moiety, differing from usual porphyrin complex. Another porphyrinoids containing phosphorus atom, phosphaporphyrins have been synthesized by Matano although they are not “phosphorus complexes”.<sup>30</sup>

As described above, many phosphorus complexes have been synthesized so far. However, the phosphorus atom exists as a phosphorus(V) state in all cases and no phosphorus(III) derivatives has been reported in the literature.

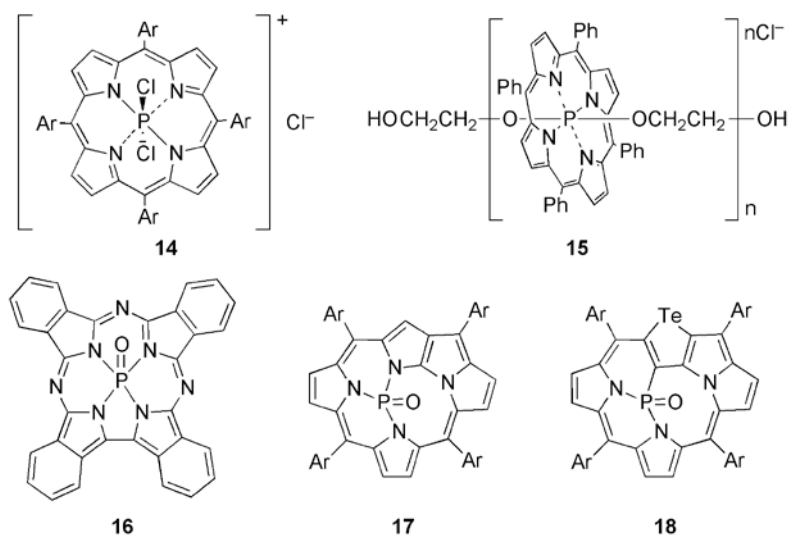


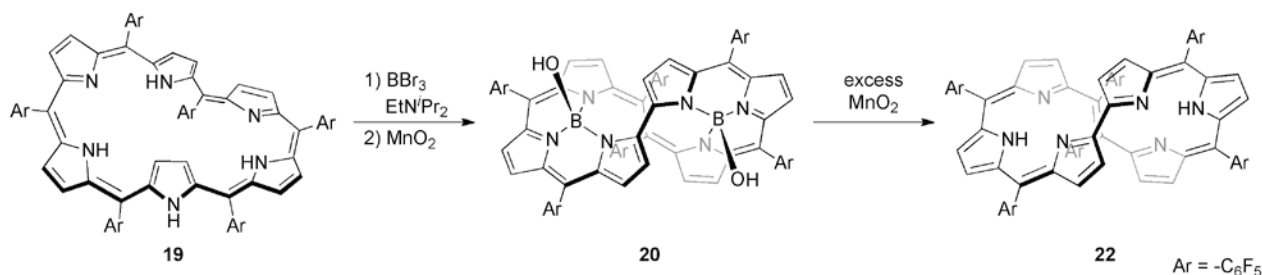
Figure 3. Representative examples of phosphorus complexes of porphyrinoids.

### 3. BORON COMPLEXES OF MESO-ARYL EXPANDED PORPHYRINS

#### 3-1. Boron Insertion Induced Skeletal Rearrangement to Hexaphyrin(2.1.1.0.1.1)

Treatment of [28]hexaphyrin(1.1.1.1.1.1) **19** with  $\text{BBr}_3$  in the presence of  $\text{EtN}^i\text{Pr}_2$  and subsequent aqueous work up, followed by oxidation with  $\text{MnO}_2$ , gave bis-boron complex **20** (Scheme 3).<sup>31</sup> The structure of **20**

was revealed by single crystal X-ray diffraction analysis to be a bis-boron complex of [28]hexaphyrin(2.1.1.0.1.1) that has a figure-of-eight conformation but has a directly connected bipyrrole unit and an *s-trans* 1,3-butadienyl linkage at the opposite position (Figure 4). Although the mechanism of skeletal rearrangement is still unclear, the transposition requires the formation of  $\alpha$ - $\alpha$  and *meso-meso* bonds and the subsequent cleavage of two *meso- $\alpha$  bonds. The axial ligands can be exchanged by a different alkoxy ligand upon treatment with an alcohol similarly to subporphyrins.*



Scheme 3. Boron insertion induced skeletal rearrangement of hexaphyrin(1.1.1.1.1.1) into hexaphyrin(2.1.1.0.1.1).

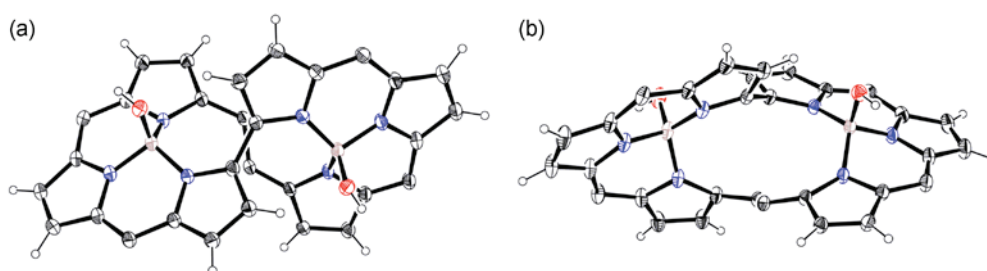
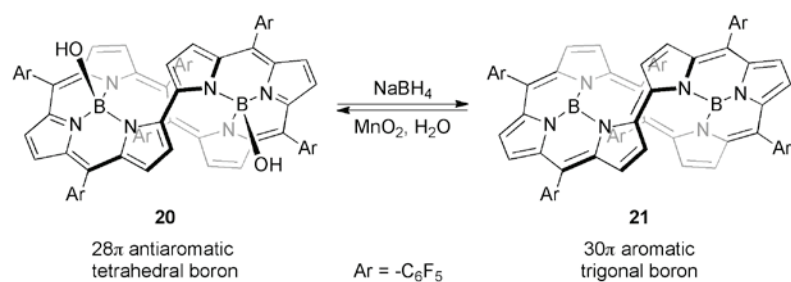


Figure 4. X-Ray crystal structure of **20**; (a) top view and (b) side view. *meso*-Pentafluorophenyl substituents are omitted for clarity.

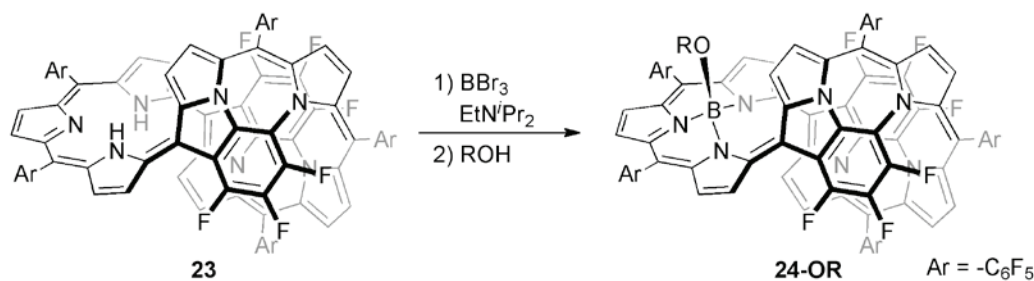
Redox interconversion between **20** and **21** was confirmed as shown in Scheme 4. Complex **21** has been characterized to be a [30]hexaphyrin(2.1.1.0.1.1) with boron atoms in a trigonal coordination environment. The  $^1\text{H}$  NMR spectrum of **20** exhibits signals of the peripheral  $\beta$ -protons at  $\delta = 8.76, 6.56, 6.23, 5.94,$  and  $5.46$  ppm with a signal at  $\delta = 4.09$  for the axial hydroxy group. These  $^1\text{H}$  NMR data indicated weak  $28\pi$  Hückel antiaromaticity. On the other hand, the  $^1\text{H}$  NMR spectrum of **21** shows six doublets at  $\delta = 7.66, 7.62, 7.53, 7.24, 7.21,$  and  $5.44$  ppm without any signal for axial ligands in line with the assigned weakly aromatic  $30\pi$  hexaphyrin structure. The reversible interconversion between **20** and **21** is interesting, in that switching between tetrahedral versus trigonal boron coordination occurs upon the change in the number of  $\pi$  electrons in the hexaphyrin(2.1.1.0.1.1) conjugation network. In addition, treatment of **20** with a large excess of  $\text{MnO}_2$  (300–400 equiv) at room temperature provided free-base [26]hexaphyrin(2.1.1.0.1.1) **22** (Scheme 3).



Scheme 4. Switching boron coordination mode by the redox interconversion of hexaphyrin(2.1.1.0.1.1).

### 3-2. Boron Complexes of Heptaphyrin and Splitting Reaction

Attempts of boron insertion into the small cavity of quadruply *N*-fused heptaphyrin **23** failed with  $\text{BF}_3 \cdot \text{OEt}_2$  but was effected upon refluxing a solution of **23** in  $\text{CH}_2\text{Cl}_2$  in the presence of  $\text{BBr}_3$  and  $\text{EtN}^i\text{Pr}_2$  (Scheme 5).<sup>32</sup> Subsequent aqueous work up provided hydroxyboron complex **24-OH**, which was converted into alkoxyboron complex **24-OR** by refluxing in the presence of alcohol. The structure of **24-O<sup>i</sup>Pr** has been revealed by single crystal X-ray diffraction analysis (Figure 5). The boron atom is bound to the three pyrroles similarly to subphthalocyanines<sup>33</sup> and subporphyrins.<sup>34</sup> This NNN-type, tripyrrolylboron-like coordination is quite rare.



Scheme 5. Boron insertion into quadruply *N*-fused heptaphyrin **23**.

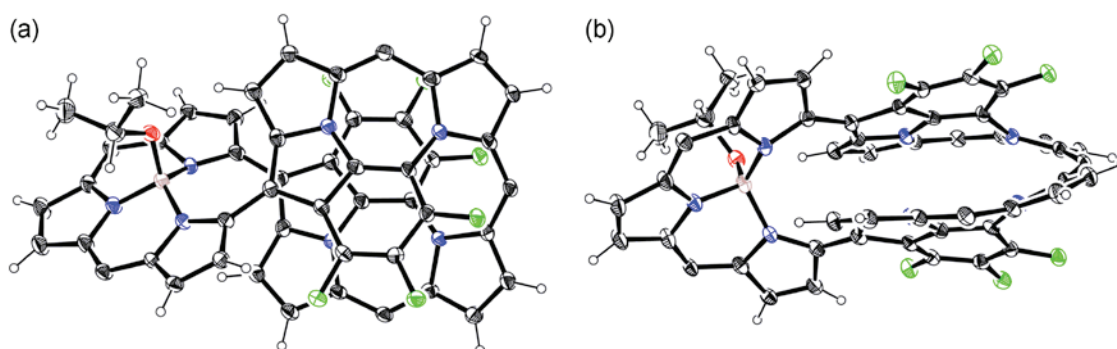
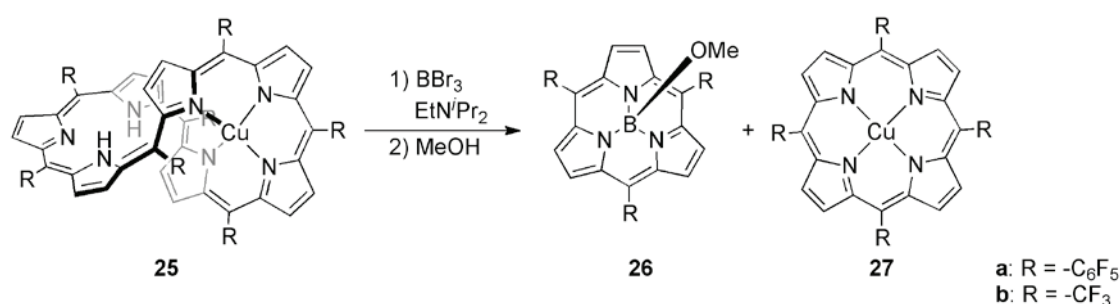


Figure 5. X-Ray crystal structure of **24-O<sup>i</sup>Pr**; (a) top view and (b) side view. Non-fused *meso*-pentafluorophenyl substituents are not shown.

Later, we found that *N*-fusion reaction of heptaphyrin **4** was suppressed by its premetalation with Zn(II) or Cu(II) ion at the hemiporphyrin-like tetrapyrrolic segment. Treatment of Zn(II) complex with BBr<sub>3</sub> or BCl<sub>3</sub> under various conditions gave a complicated mixture containing free-base **4**, a B(III)-Zn(II) dinuclear complex, and subporphyrin **26**. However, the yield of **26** is quite low (<1%). On the other hand, treatment of Cu(II) complex **25a** with BBr<sub>3</sub> in the presence of EtN<sup>*i*</sup>Pr<sub>2</sub> at room temperature provided subporphyrin **26a** and Cu(II) porphyrin **27a** in 36 and 13% yield, respectively (Scheme 6).<sup>35</sup> This splitting reaction is synthetically useful because the subporphyrin **26a** cannot be obtained by the usual subporphyrin synthesis. Similar extrusion reaction of *meso*-trifluoromethyl heptaphyrin **25b** provided subporphyrin **26b**.<sup>36</sup>



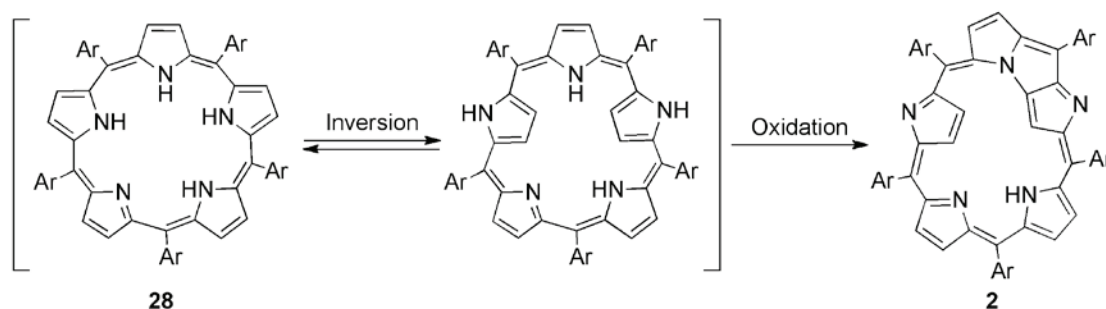
Scheme 6. Splitting reaction of heptaphyrin Cu(II) complex **25** into subporphyrin **26** and porphyrin Cu(II) complex **27**.

## 4. PHOSPHORUS COMPLEXES OF MESO-ARYL EXPANDED PORPHYRINS

### 4-1. *N*-Fused Pentaphyrin (NFP<sub>5</sub>)

#### 4-1-1. General Properties

Generally, *meso*-aryl-substituted pentaphyrin(1.1.1.1.1) **28** was obtained by acid-catalyzed condensation as only *N*-fused forms **2** in contrast to  $\beta$ -alkyl pentaphyrin reported by Gossaur.<sup>37</sup> This *N*-fused structure was formed via inversion of pyrrole ring followed by oxidation, because of severe steric repulsion (Scheme 7).<sup>38</sup> As a rare case, mono-*meso*-free pentaphyrin **29** was reported quite recently.<sup>39</sup> Non-fused **29** possesses an inward-pointing *meso*-carbon bridge, preventing the inversion of pyrrole rings (Figure 6).



Scheme 7. *N*-Fusion reaction of *meso*-aryl pentaphyrin(1.1.1.1.1) **28** to **2**.



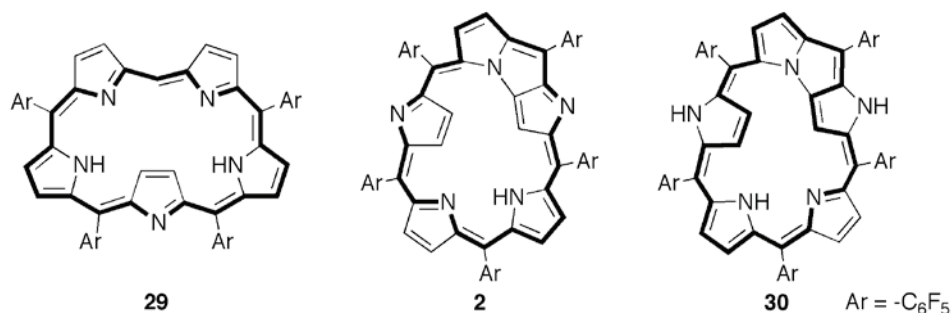


Figure 6. *meso*-Aryl pentaphyrin(1.1.1.1.1) free-bases.

Pentaphyrin has two stable redox states with  $22\pi$ - and  $24\pi$ -electronic systems,  $[22]\text{NFP}_5$  **2** and  $[24]\text{NFP}_5$  **30**, respectively (Figure 6). Pentaphyrin **2** can easily be reduced to **30** with  $\text{NaBH}_4$ , and **30** is quantitatively oxidized back to **2** by treatment with DDQ. X-Ray crystal structures reveal that both **2** and **30** have a fused tricyclic structure, a dipyrromethene moiety, and an outward-pointing pyrrole (Figure 7). Except for the inverted pyrrole that is tilted significantly, the entire structure of **2** is almost planar so that a strong diatropic ring current effect arising from the  $22\pi$  aromaticity is observed in the  $^1\text{H}$  NMR spectrum. On the other hand, **30** exhibits weak antiaromatic character due to its  $24\pi$ -electron state.

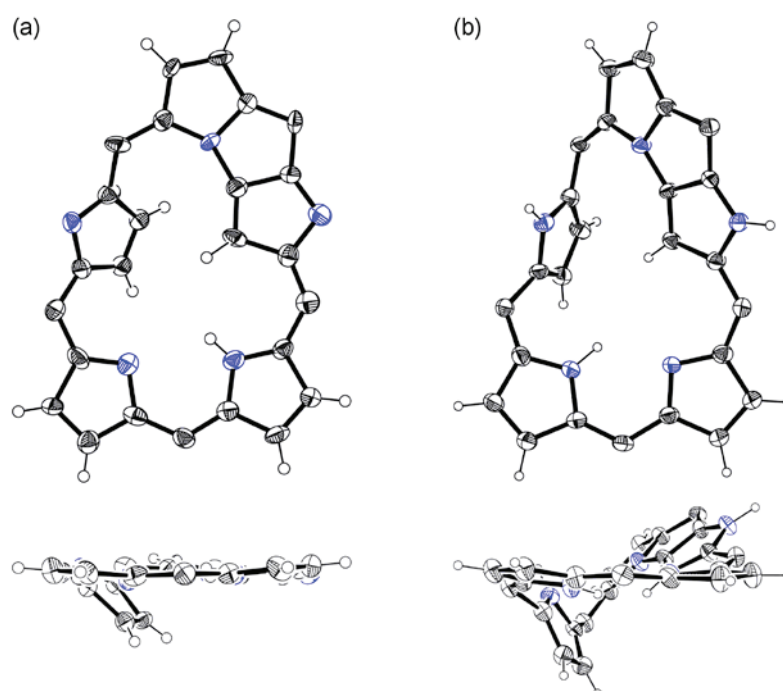
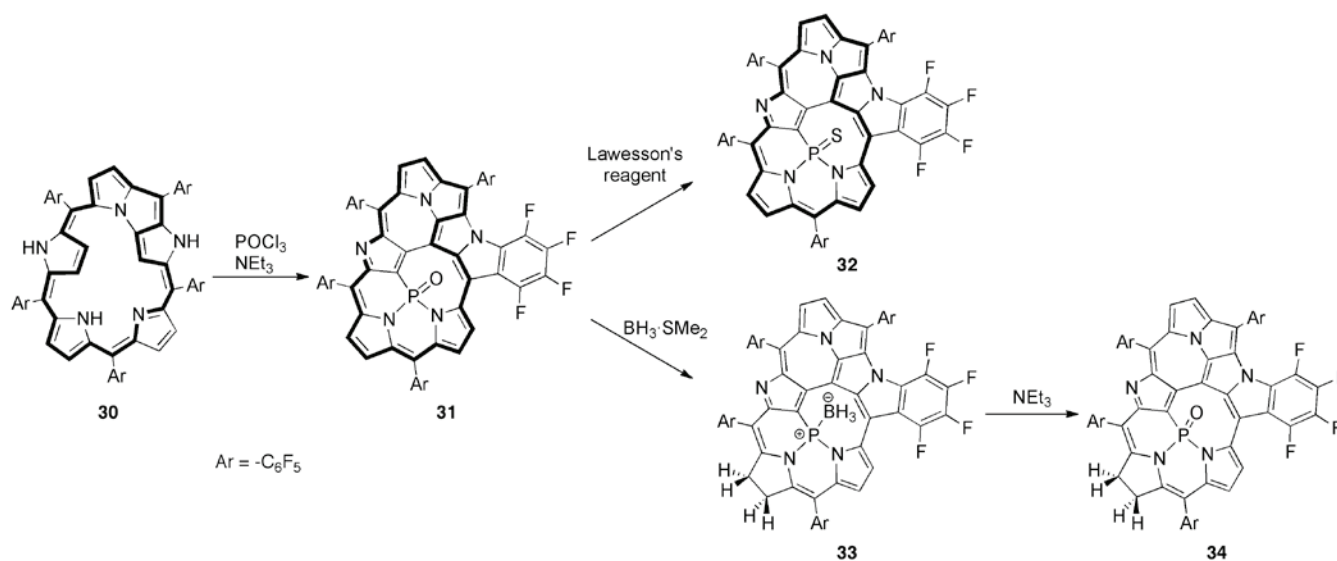


Figure 7. X-Ray crystal structures of (a) **2** and (b) **30**; top views (top) and side views (bottom). *meso*-Aryl substituents are not shown.

#### 4-1-2. Phosphorus Complexes of Triply Fused $[24]$ Pentaphyrin

The reaction of **30** and  $\text{POCl}_3$  in the presence of triethylamine provided the  $\text{P}=\text{O}$  complex **31** in 66% yield (Scheme 8).<sup>40</sup> The crystal structure of **31** revealed the inserted phosphorus atom bound to two nitrogen

atoms and one carbon atom (Figure 8a). At the same time, *N*-fusion reaction between nitrogen atom N(5) and pentafluorophenyl substituent at C(55), and C–C bond formation between C(13) and C(23) occurred to form a triply fused structure. The  $^1\text{H}$  NMR spectrum of **31** displays five peaks due to the  $\beta$ -protons in the range of 6.35–4.34 ppm, indicating moderate antiaromaticity derived from  $24\pi$ -electron state. The antiaromaticity likely originates from its highly rigid planar conformation forced by the phosphorus incorporation and triply fused structure.



Scheme 8. Syntheses of phosphorus complexes of multiply fused pentaphyrin.

The P=O moiety of **31** can be converted to different phosphorus states (Scheme 8). Complex **31** was converted to P=S complex **32** by the reaction with Lawesson's reagent in 84% yield. Complex **32** has also a highly rigid planar structure and exhibits distinct antiaromaticity. In addition, complex **31** was reduced with BH<sub>3</sub>·SMe<sub>2</sub> to provide phosphine-borane (P–BH<sub>3</sub>) complex **33** in 54% yield. X-Ray diffraction analysis of **33** revealed a C(7)–C(8) single bond with bond length of 1.544(5) Å, which was distinctly longer than those of C(2)–C(3) and C(17)–C(18) double bonds; 1.390(5) and 1.375(5) Å, respectively (Figure 8c). The  $^1\text{H}$  NMR spectrum of **33** displays four peaks due to the  $\beta$ -protons of the reduced pyrrole B at 2.65, 2.53, 2.37, and 2.18 ppm, and four peaks due to the  $\beta$ -protons of the pyrroles A and D at 7.22, 6.96, 6.33, and 5.57 ppm. These data indicate nonaromatic character derived from the interruption of macrocyclic conjugation at reduced pyrrole B.

Using these three phosphorus complexes, the realization of free phosphorus(III) species was attempted. However, neither the reduction of **31** with silane reducing reagents nor desulfurization of **32** with electron-rich phosphines or Raney Nickel gave the desired phosphorus(III) compounds. On the other hand, the attempt at removal of borane from **33** provided the chlorin-type P=O complex **34**, no free phosphorus(III) compounds was obtained (Scheme 8). Therefore, it is conceivable that a free P(III) species is quite unstable toward oxygenation. In this regard, P–BH<sub>3</sub> complex **33** can be regarded as a

phosphorus(III) complex, which is rare in the chemistry of phosphorus porphyrinoid.

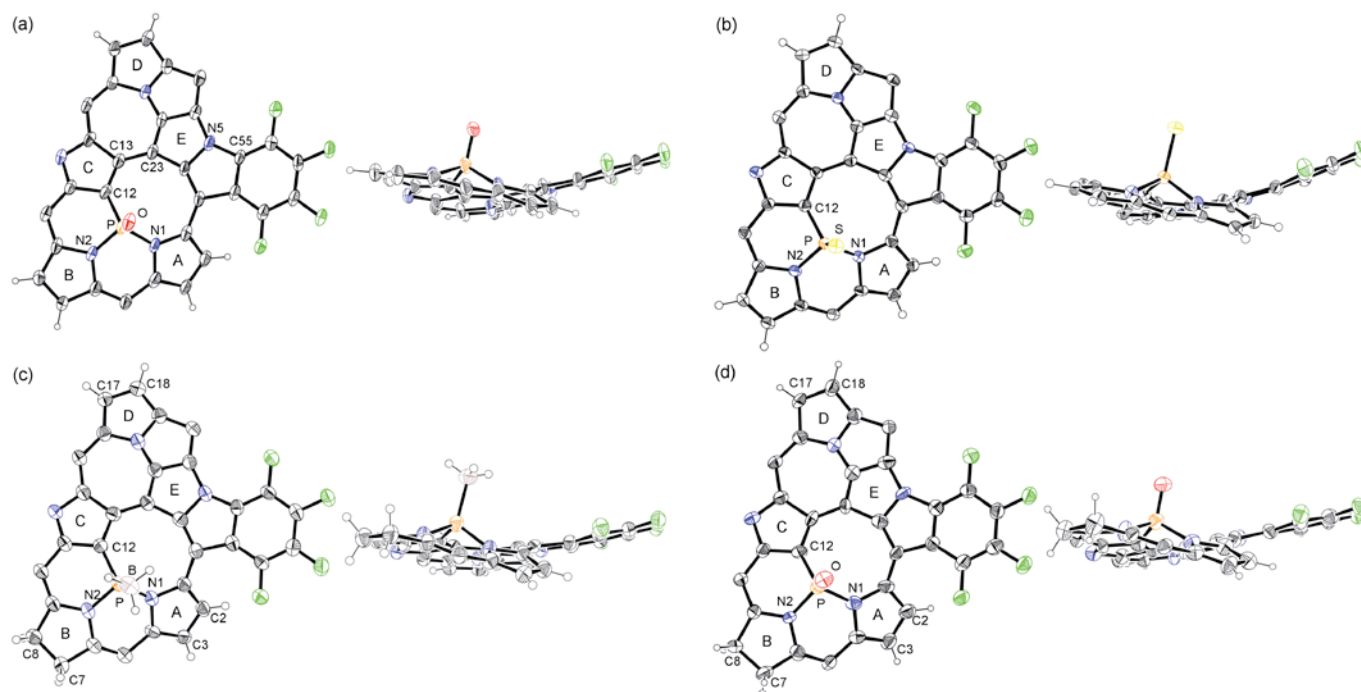


Figure 8. X-Ray crystal structures of (a) **31**, (b) **32**, (c) **33** and (d) **34**; top views (left) and side views (right). *meso*-Pentafluorophenyl substituents are omitted for clarity.

## 4-2. Hexaphyrin

### 4-2-1. General Properties

[26]Hexaphyrin(1.1.1.1.1.1) **3**, which was first synthesized by Cavaleiro and co-workers,<sup>41</sup> is one of the most studied expanded porphyrins. Hexaphyrin **3** was obtained as a major product in 16–20% yield by modified Rothmund-Lindsey protocol as an oxidized form with  $26\pi$ -electron system.<sup>8</sup> [26]Hexaphyrin **3** is easily reduced to [28]hexaphyrin **19** upon treatment with  $\text{NaBH}_4$ , and **19** can be oxidized back to **3** (Scheme 9). Depending on the substituents, [26]hexaphyrins(1.1.1.1.1.1) take various conformations such as rectangle (**3**),<sup>11,41</sup> dumbbell (**35**),<sup>42</sup> figure-of-eight (**36**),<sup>43</sup> and triangle (**37-MSA**)<sup>44</sup> (Figure 9). Most of *meso*-aryl [26]hexaphyrins adopt a planar rectangular conformation with two inverted pyrrole rings, which allow its strong  $26\pi$  aromaticity. On the other hand, [28]hexaphyrin exists as an equilibrium of rapid interconversion between twisted Möbius aromatic conformations and rectangular antiaromatic conformation in solution at ambient temperature (Figure 10).<sup>45</sup> These rapid interconversions were frozen at low temperature ( $-100\text{ }^\circ\text{C}$ ), so that the  $^1\text{H}$  NMR spectrum exhibits distinct aromaticity because of the predominant contribution of a single Möbius conformation.

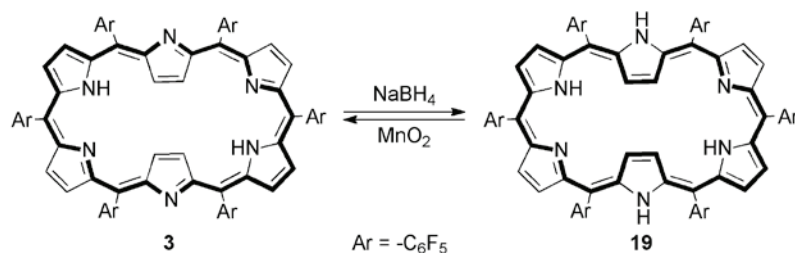
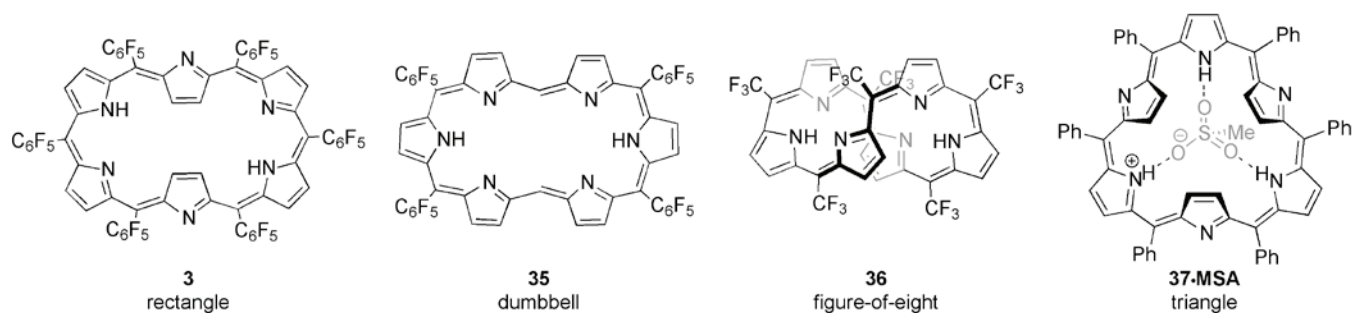
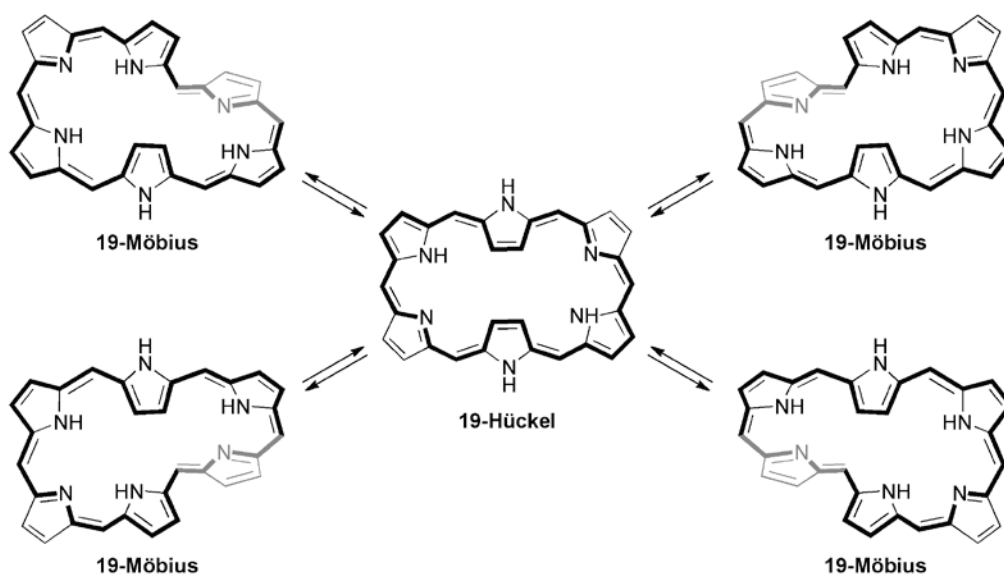
Scheme 9. Redox behavior of hexaphyrin **3** and **19**.

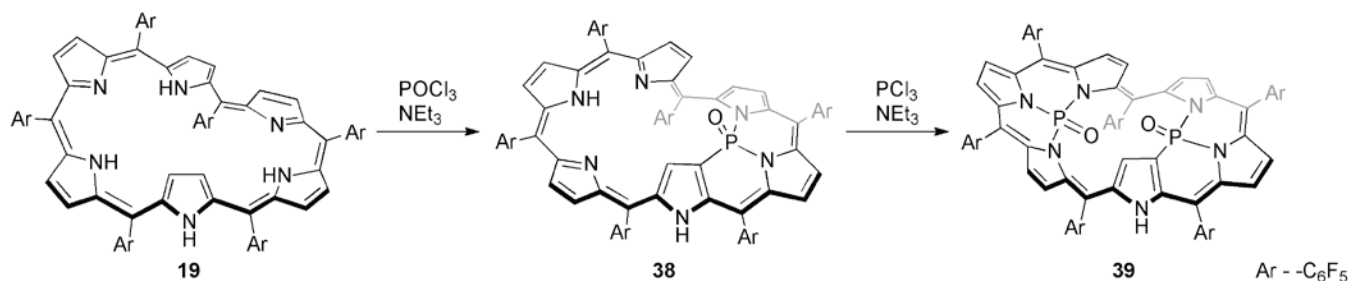
Figure 9. Various conformations of [26]hexaphyrins.

Figure 10. Equilibrium of *meso*-aryl [28]hexaphyrin **19**. *meso*-Aryl substituents are not shown.

#### 4-2-2. Möbius Aromatic and Antiaromatic Phosphorus Complexes of Hexaphyrin

The reaction of [28]hexaphyrin **19** with POCl<sub>3</sub> gave mono-phosphorus complex **38** in 65% yield (Scheme 10).<sup>46</sup> The twisted Möbius structure of **38** was revealed by X-ray diffraction analysis, in which the phosphoryl moiety was bound to the two nitrogen atoms of the pyrrole units A and B, and one carbon atom of the pyrrole unit C (Figure 11a). The <sup>31</sup>P NMR spectrum of **38** shows a signal at -11.99 ppm, which is consistent with a P=O moiety. The <sup>1</sup>H NMR spectrum of **38** displays ten signals of outer β-protons in the range δ = 7.75–6.53 ppm and a doublet signal of inner β-proton of the pyrrole unit C at δ

= 2.99 ppm. The difference between the chemical shifts ( $\Delta\delta$ ) of the most shielded and deshielded  $\beta$ -protons is 4.76 ppm, indicating a diatropic ring current despite the large dihedral angle ( $65^\circ$ ) along its  $\pi$  conjugation.



Scheme 10. Synthesis of phosphorus complexes of hexaphyrins.

Further treatment of **38** with PCl<sub>3</sub> provided bis-phosphorus complex **39** in 46% yield (Scheme 10). The structure of bis-phosphorus complex **39** was also determined by X-ray diffraction analysis to be a twisted Möbius conformation (Figure 11b). The additional P=O moiety was bound to the three nitrogen atoms of the pyrrole units D, E, and F. The <sup>31</sup>P NMR spectrum of **39** shows two signals at -5.67 and -7.70 ppm. Complex **39** was assigned as a reduced [30]hexaphyrin by high-resolution ESI-TOF-MS and charge consideration. This highly reduced electron state is probably stabilized by the two electron-withdrawing P=O moieties. The <sup>1</sup>H NMR spectrum of **39** exhibits a remarkably deshielded signal at  $\delta = 11.14$  ppm that corresponds to the inner  $\beta$ -protons of pyrrole unit C, and ten signals in the range  $\delta = 6.72$ – $5.54$  ppm that correspond to the outer  $\beta$ -protons. These data indicate a paratropic ring current.

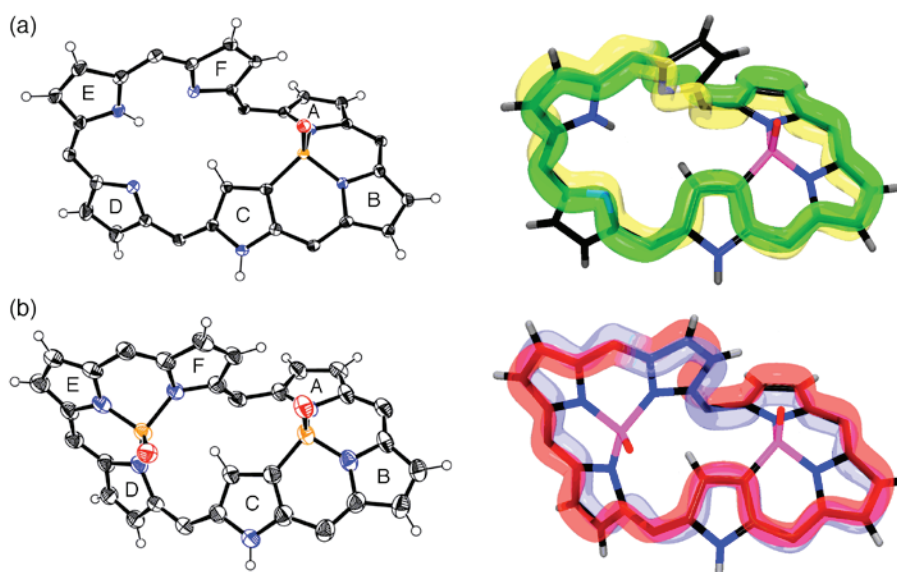


Figure 11. X-Ray crystal structures (left) and schematic representations of molecular topologies (right) of (a) **38** and (b) **39**. *meso*-Aryl substituents are omitted for clarity.

The UV/vis absorption spectrum of **38** exhibits an intense Soret-like band at 588 nm and broad Q-like bands at 876 and 1055 nm. Moreover, **38** exhibits a fluorescence band at 1090 nm as a mirror image of the corresponding absorption spectrum (Figure 12). In contrast, the UV/vis absorption spectrum of **39** shows ill-defined Soret-like bands and broad, weak near-IR bands. Furthermore, **39** shows no fluorescence emission. These absorption and emission behaviors of **39** are characteristic of antiaromatic expanded porphyrins. NICS values at the gravity center of **38** and **39** were calculated to be  $-8.25$  and  $+3.65$  ppm, respectively in line with the assignments of Möbius aromatic and antiaromatic characters. It is worthy to note that **39** is the first structurally well-defined Möbius antiaromatic molecule.

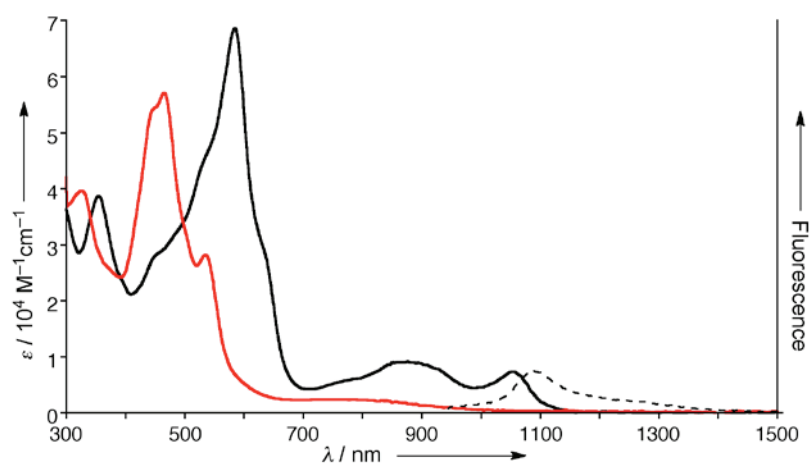
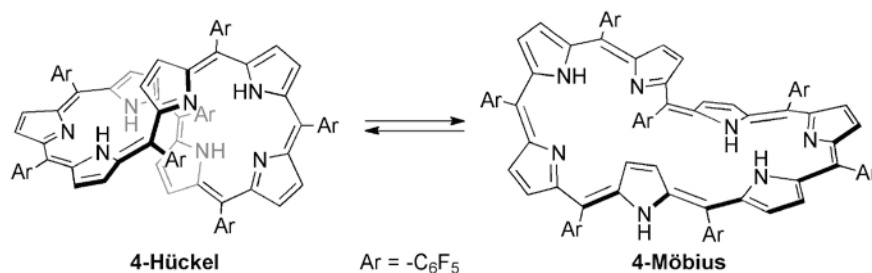


Figure 12. UV/Vis absorption spectra of **38** (black) and **39** (red) in  $\text{CH}_2\text{Cl}_2$ . The fluorescence emission spectrum of **38** is shown by a dotted line.

### 4-3. Heptaphyrin

#### 4-3-1. General Properties

*meso*-Aryl heptaphyrins(1.1.1.1.1.1.1) are obtained by acid-catalyzed condensation with usually  $32\pi$  electron state as the most stable form. *meso*-Pentafluorophenyl [32]heptaphyrin **4** takes a figure-of-eight Hückel antiaromatic conformation in nonpolar solvents such as hexane, toluene, and  $\text{CH}_2\text{Cl}_2$  (Figure 13a).<sup>47</sup> The conformation of **4** depends on the polarity of the solvent, **4** takes a twisted Möbius aromatic conformation in polar solvents such as acetone (Scheme 11). In contrast to **4**, *meso*-(2,6-dichlorophenyl) [32]heptaphyrin **40** takes a twisted Möbius conformation even in nonpolar solvents such as hexane. Its X-ray crystal structure shows a singly twisted Möbius structure with a smoothly conjugated pathway, which is consistent with its aromaticity confirmed by  $^1\text{H}$  NMR and UV/vis absorption (Figure 13b).



Scheme 11. Switching topology between figure-of-eight Hückel antiaromatic conformer and Möbius aromatic conformer of **4**.

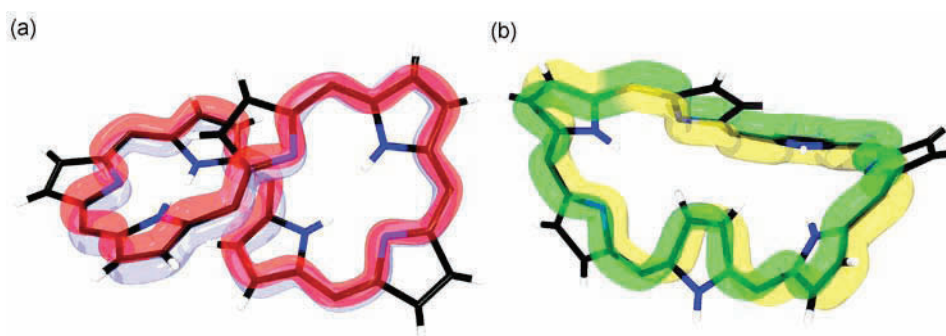
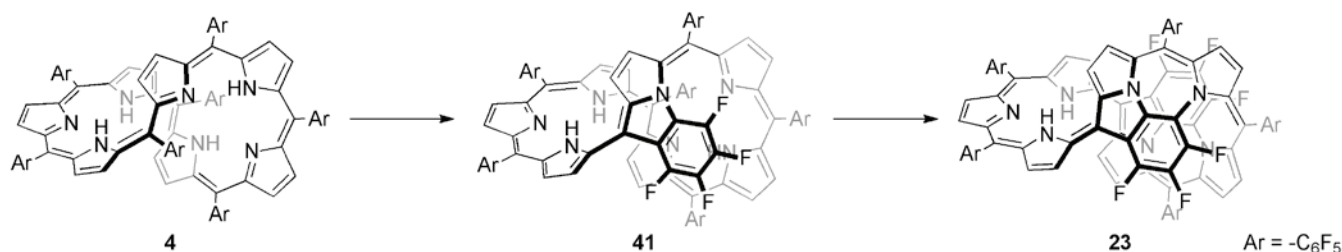


Figure 13. (a) Hückel conformation based on the crystal structure of **4**, and (b) Möbius conformation based on the crystal structure of **40**. *meso*-Aryl substituent are not shown.

*meso*-Pentafluorophenyl [32]heptaphyrin **4** underwent *N*-fusion reaction quantitatively to form singly *N*-fused heptaphyrin **41** just on standing in solution.<sup>32</sup> Further *N*-fusion reactions were induced by heating of a toluene solution of **41** at reflux, and then heating of a DMF solution with NaH provided quadruply *N*-fused heptaphyrin **23** as a rare  $34\pi$ -electron species (Scheme 12). In addition, the figure-of-eight structure of **23** is rigid enough to separate two enantiomers.



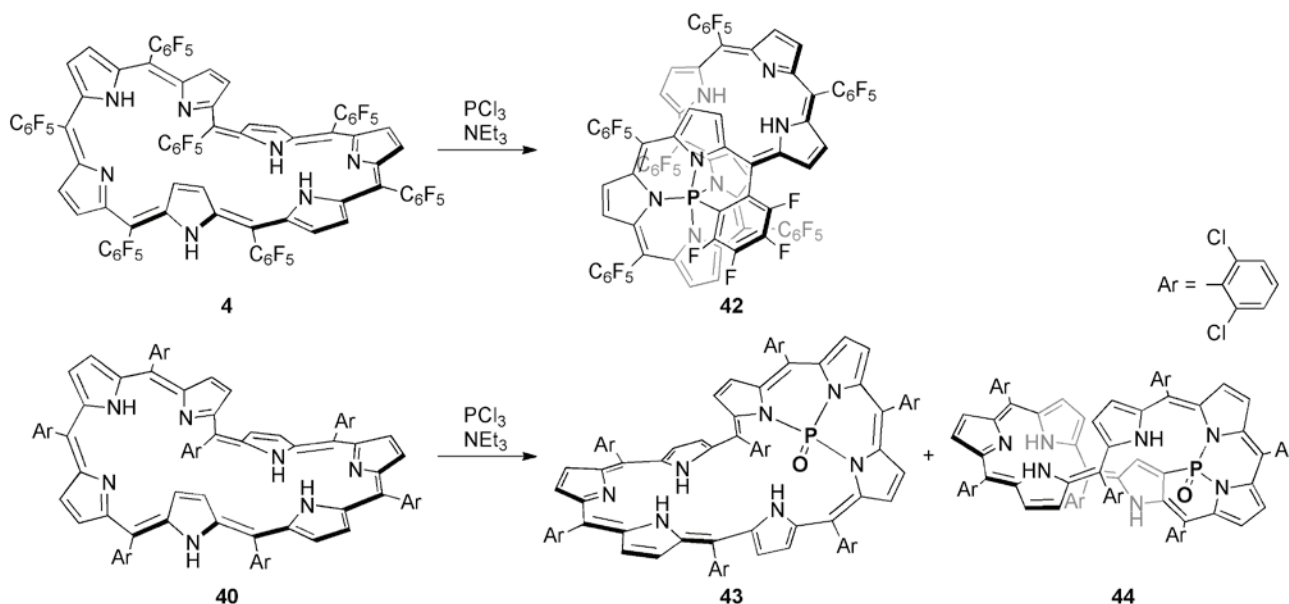
Scheme 12. *N*-Fusion reaction of *meso*-pentafluorophenyl heptaphyrin(1.1.1.1.1.1.1) **4**.

### 4-3-2. Hückel Aromatic and Möbius Antiaromatic Phosphorus Complexes of Heptaphyrin

Treatment of *meso*-pentafluorophenyl [32]heptaphyrin **4** with PCl<sub>3</sub> gave phosphorus complex **42** in 46% yield (Scheme 13).<sup>48</sup> The crystal structure of **42** revealed a figure-of-eight conformation with

penta-coordinated phosphorus atom bound to the four nitrogen atoms of the pyrrole rings A, B, C and D, and one *ortho*-carbon atom of a pentafluorophenyl group in a trigonal bipyramidal manner (Figure 14a). The  $^{31}\text{P}$  NMR spectrum of **42** shows a signal at  $-82.41$  ppm, which is consistent with the penta-coordination geometry.<sup>49</sup> Complex **42** is regarded as a weakly  $34\pi$  aromatic molecule from its  $^1\text{H}$  NMR and UV/vis absorption spectra.

On the other hand, treatment of *meso*-(2,6-dichlorophenyl) [32]heptaphyrin **40** with  $\text{PCl}_3$  provided two phosphorus complexes **43** and **44** in 49 and 35% yield, respectively (Scheme 13). The ratio of two complexes is dependent on reaction temperature. While complex **43** is a major product at low temperature ( $\mathbf{43}/\mathbf{44} = 1.9/1$  at  $0^\circ\text{C}$ ), complex **44** is a major product at high temperature ( $\mathbf{43}/\mathbf{44} = 1/4.1$  at  $60^\circ\text{C}$ ). These results indicated that **43** is a kinetic product. This has been more clearly shown that heating of **43** in acetonitrile led to quantitative conversion to **44**.



Scheme 13. Synthesis of phosphorus complexes of heptaphyrins.

These two phosphorus complexes **43** and **44** are also assigned as [34]heptaphyrin by high resolution ESI-TOF-MS. The crystal structure of **43** revealed a twisted Möbius structure, in which the phosphorus atom was bound to the three nitrogen atoms of the pyrrole rings A, B and C as a  $\text{P}=\text{O}$  moiety (Figure 14b). The UV/vis absorption spectrum of **43** has an ill-defined Soret-like band, and weak and broad bands in near-IR region, which are characteristic of antiaromatic expanded porphyrins. Moreover, the  $^1\text{H}$  NMR spectrum of **43** displays signals due to the inner pyrrolic  $\beta$ -protons in the pyrrole rings A and D at 7.96 and 7.60 ppm, which are distinctly deshielded from the other outer  $\beta$ -protons that appear in the range of 6.51–5.51 ppm, indicating a weak paratropic ring current. From these spectroscopic studies, complex **43** is characterized as a Möbius antiaromatic molecule.



The other complex **44** was determined to take a figure-of-eight Hückel structure on the basis of X-ray diffraction analysis (Figure 14c). The P=O moiety was bound to the two nitrogen atoms of the pyrrole rings B and C, and one  $\beta$ -carbon atom of the pyrrole ring D. The complex **44** was assigned as a  $34\pi$  Hückel aromatic molecule. The  $^1\text{H}$  NMR spectrum is very broad at room temperature, probably due to conformational flexibility, but became sharpened at  $-60\text{ }^\circ\text{C}$ , exhibiting a doublet at 1.98 ppm due to the inner  $\beta$ -proton in the pyrrole D and twelve signals due to other  $\beta$ -protons in a range of 6.91–3.80 ppm. The difference of chemical shifts ( $\Delta\delta$ ) is relatively large (4.93 ppm), indicating the presence of a diatropic ring current.

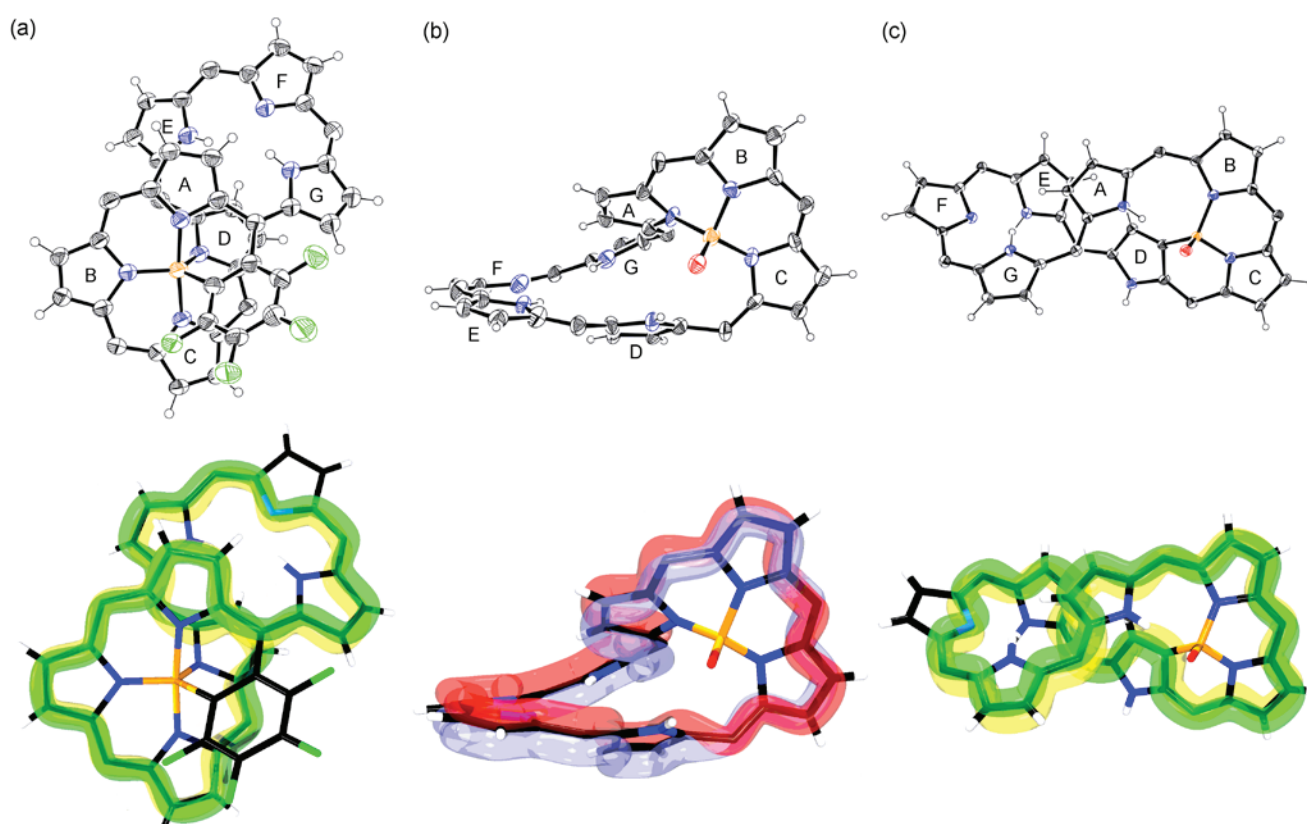


Figure 14. X-Ray crystal structures (top) and schematic representations of molecular topologies (bottom) of (a) **42**, (b) **43** and (c) **44**. *meso*-Aryl substituents are omitted for clarity.

## 4-4. Octaphyrin

### 4-4-1. General Properties

Since *meso*-aryl octaphyrin(1.1.1.1.1.1.1.1) has a large conjugation network, it possesses three different redox states with  $34\pi$ -,  $36\pi$ -, and  $38\pi$ -electrons (Scheme 14). In the crystal structure, [36]octaphyrin **5** that is the most stable form, adopts a figure-of-eight conformation, consisting of two porphyrin-like tetrapyrrolic “hemi-macrocycles”.<sup>8</sup> However, the  $^1\text{H}$  NMR spectrum of **5** indicates its nonaromatic nature. [36]Octaphyrin **5** is easily converted to [34]octaphyrin **45** by the oxidation with DDQ and to

[38]octaphyrin **46** by the reduction with  $\text{NaBH}_4$  quantitatively. The structure of **45** revealed to be a figure-of-eight conformation with two inverted pyrrole rings (Figure 15). Contrary to **5**, the  $^1\text{H}$  NMR spectrum of **45** displays a diatropic ring current effect, indicating a distinct  $34\pi$  aromaticity. While [38]octaphyrin **46** also exhibits a  $38\pi$ -aromatic character, the structure of **46** has not been determined yet.



Scheme 14. Redox interconversions of *meso*-aryl octaphyrins.

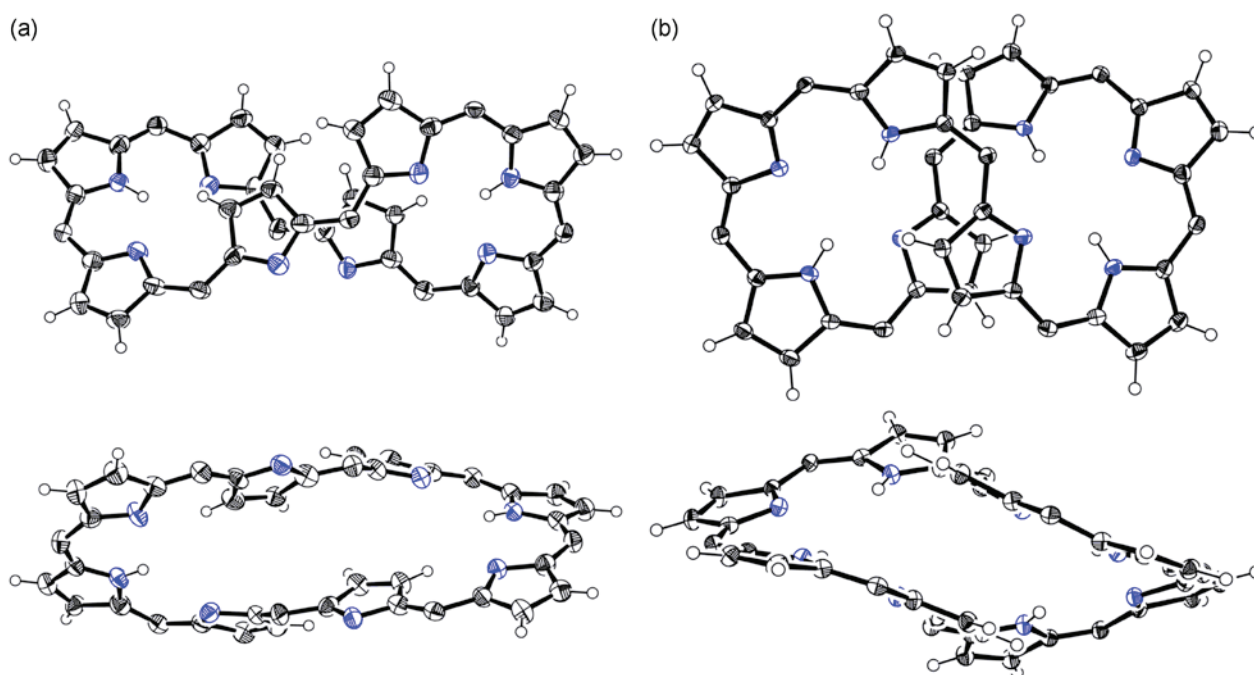
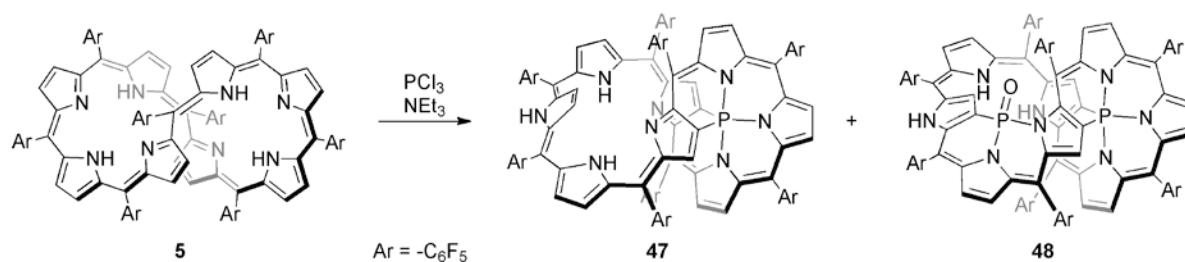


Figure 15. X-Ray crystal structures of (a) **45** and (b) **5**; top views (top) and side views (bottom). *meso*-Aryl substituents are omitted for clarity.

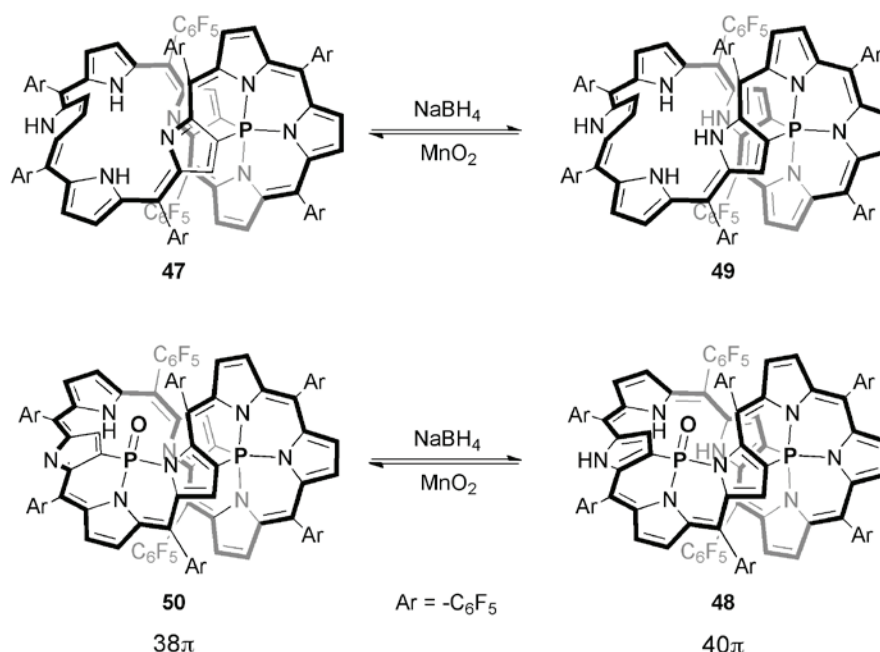
#### 4-4-2. Phosphorus Complexes of Octaphyrin: Expanded Isophlorin

The reaction of [36]octaphyrin **5** with  $\text{PCl}_3$  in the presence of triethylamine gave mono-phosphorus complex **47** and bis-phosphorus complex **48** in 43 and 9% yield, respectively (Scheme 15).<sup>50</sup> In the presence of an additional small amount of water and by heating at  $50\text{ }^\circ\text{C}$ , bis-phosphorus complex **48** was obtained as a major product in 35% yield along with **47**.



Scheme 15. Synthesis of phosphorus complexes of octaphyrin.

The structure of **47** was revealed by X-ray diffraction analysis to be a figure-of-eight structure with penta-coordinated phosphorus atom, which was bound to the three nitrogen atoms of the pyrroles F, G, H and two  $\beta$ -carbon atoms of the pyrroles A and E in a trigonal bipyramidal manner (Figure 16a). The  $^{31}\text{P}$  NMR spectrum shows a signal at  $-85.59$  ppm, which is consistent with penta-coordination.<sup>49</sup> The UV/vis absorption spectrum shows a Q-like band derived from  $38\pi$  aromaticity at 1620 nm. Complex **47** can be reduced with  $\text{NaBH}_4$  to corresponding  $40\pi$ -electron species **49**, which is smoothly oxidized to **47** (Scheme 16). However, [40]octaphyrin **49** is unstable and readily oxidized back to **47**, even when it is stored in the solid-state because of its highly reduced electron state.

Scheme 16. Redox interconversions of  $38\pi$  and  $40\pi$  octaphyrins.

The crystal structure of bis-phosphorus complex **48** was also a figure-of-eight structure, in which the additional  $\text{P}=\text{O}$  moiety was bound to the two nitrogen atoms of the pyrroles A, B and one  $\beta$ -carbon atom of the pyrrole C. The  $^{31}\text{P}$  NMR spectrum shows a new signal due to the additional  $\text{P}=\text{O}$  moiety at  $-9.80$  ppm. From  $^1\text{H}$  NMR, MS and crystal structure, **48** is characterized as a [40]octaphyrin bis-phosphorus

complex. The oxygen source of the P=O moiety of **48** is a small amount of water, which has been confirmed by synthesis of  $^{18}\text{O}$ -labelled **48** using  $\text{H}_2^{18}\text{O}$ . Similar to the redox behaviors of **47** and **49**, the oxidation of **48** gave aromatic [38]octaphyrin complex **50**, and it is reduced back to **48** with  $\text{NaBH}_4$ . In contrast to **49**, bis-phosphorus complex **48** is stable under ambient condition and can be stored over several months without any oxidation in the solid state. The increase of stability is derived from electron-withdrawing effect of the P=O moiety. Importantly, this bis-phosphorus complex **48** is the first stable [40]octaphyrin, in other words, expanded isophlorin.

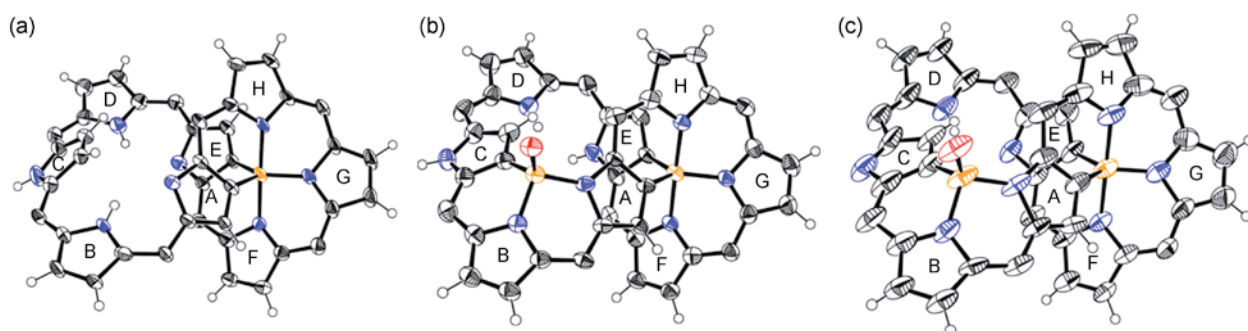


Figure 16. X-Ray crystal structures of (a) **47**, (b) **48** and (c) **50**. *meso*-Aryl substituents are omitted for clarity.

## 5. CONCLUSION

The boron insertion into *meso*-aryl expanded porphyrins triggered novel skeletal rearrangements such as the methine carbon transposition from [28]hexaphyrin(1.1.1.1.1.1) to [28]hexaphyrin(2.1.1.0.1.1) and the splitting reaction of a putative B(III)-Cu(II) complex of [34]heptaphyrin into subporphyrin and Cu(II) porphyrin. Similarly, the phosphorus insertion into *N*-fused pentaphyrin induced the multiple more fusion reactions. Interestingly, the phosphorus complexes can take fully reduced electron states, such as [24]pentaphyrin, [30]hexaphyrin, [34]heptaphyrin and [40]octaphyrin as “expanded isophlorins”, since the incorporated phosphorus atoms exist as strongly electron-withdrawing phosphorus(V) states, hence stabilizing the reduced states by their electron-withdrawing effects. Most importantly, the phosphorus insertions into [30]hexaphyrin and [34]heptaphyrin allowed the formation of the stable Möbius antiaromatic molecules as the first examples of structurally well-defined species.

## ACKNOWLEDGEMENTS

This work was supported by Grants-in-Aid (No. 22245006(A) and 20108001 “ $\pi$ -space”) for Scientific Research from MEXT. T. H. acknowledges a JSPS Fellowship for Young Scientists.

## REFERENCES

1. a) 'The Porphyrin Handbook,' Vol. 1–10, ed. by K. M. Kadish, K. M. Smith, and R. Guilard, Academic Press, San Diego, 2000; b) A. Jasat and D. Dolphin, *Chem. Rev.*, 1997, **97**, 2267; c) T. D.

- Lash, *Angew. Chem. Int. Ed.*, 2000, **39**, 1763; d) H. Furuta, H. Maeda, and A. Osuka, *Chem. Commun.*, 2002, 1795; e) J. L. Sessler and D. Seidel, *Angew. Chem. Int. Ed.*, 2003, **42**, 5134; f) K. Chandrashekar and S. Venkatraman, *Acc. Chem. Res.*, 2003, **36**, 676; g) A. Ghosh, *Angew. Chem. Int. Ed.*, 2004, **43**, 1918; h) M. Stępień, N. Sprutta, and L. Latos-Grażyński, *Angew. Chem. Int. Ed.*, 2011, **50**, 4288; i) S. Saito and A. Osuka, *Angew. Chem. Int. Ed.*, 2011, **50**, 4342; j) A. Osuka and S. Saito, *Chem. Commun.*, 2011, **47**, 4330.
- a) S. Shimizu and A. Osuka, *Eur. J. Inorg. Chem.*, 2006, 1319; b) J. L. Sessler and E. Tomat, *Acc. Chem. Res.*, 2007, **40**, 371.
  - a) S. Mori, J.-Y. Shin, S. Shimizu, F. Ishikawa, H. Furuta, and A. Osuka, *Chem. Eur. J.*, 2005, **11**, 2417; b) S. Mori and A. Osuka, *J. Am. Chem. Soc.*, 2005, **127**, 8030.
  - a) T. K. Ahn, J. H. Kwon, D. Y. Kim, D. W. Cho, D. H. Jeong, S. K. Kim, M. Suzuki, S. Shimizu, A. Osuka, and D. Kim, *J. Am. Chem. Soc.*, 2005, **127**, 12856; b) Z. S. Yoon, J. H. Kwon, M.-C. Yoon, M. K. Koh, S. B. Noh, J. L. Sessler, J. T. Lee, D. Seidel, A. Aguilar, S. Shimizu, M. Suzuki, A. Osuka, and D. Kim, *J. Am. Chem. Soc.*, 2006, **128**, 14128; c) J. M. Lim, Z. S. Yoon, J.-Y. Shin, K. S. Kim, M.-C. Yoon, and D. Kim, *Chem. Commun.*, 2009, 261.
  - a) M. Suzuki and A. Osuka, *J. Am. Chem. Soc.*, 2007, **129**, 464; b) M. Suzuki and A. Osuka, *Angew. Chem. Int. Ed.*, 2007, **46**, 5171.
  - a) Y. Tanaka, W. Hoshino, S. Shimizu, K. Youfu, N. Aratani, N. Maruyama, S. Fujita, and A. Osuka, *J. Am. Chem. Soc.*, 2004, **126**, 3046; b) Y. Tanaka, H. Shinokubo, Y. Yoshimura, and A. Osuka, *Chem. Eur. J.*, 2009, **15**, 5674; c) Y. Tanaka, H. Mori, T. Koide, H. Yorimitsu, N. Aratani, and A. Osuka, *Angew. Chem. Int. Ed.*, 2011, **50**, 11460; d) H. Mori, N. Aratani, and A. Osuka, *Chem. Asian J.*, 2012, **7**, 1340.
  - a) M. Stępień, L. Latos-Grażyński, N. Sprutta, P. Chawalisz, and L. Szterenber, *Angew. Chem. Int. Ed.*, 2007, **46**, 7869; b) Y. Tanaka, S. Saito, S. Mori, N. Aratani, H. Shinokubo, N. Shibata, Y. Higuchi, Z. S. Yoon, K. S. Kim, S. B. Noh, J. K. Park, D. Kim, and A. Osuka, *Angew. Chem. Int. Ed.*, 2008, **47**, 681; c) J. K. Park, Z. S. Yoon, M.-C. Yoon, K. S. Kim, S. Mori, J.-Y. Shin, A. Osuka, and D. Kim, *J. Am. Chem. Soc.*, 2008, **130**, 1824; d) M. Inoue, K. S. Kim, M. Suzuki, J. M. Lim, J.-Y. Shin, D. Kim, and A. Osuka, *Angew. Chem. Int. Ed.*, 2009, **48**, 6687; e) J. M. Lim, J.-Y. Shin, Y. Tanaka, S. Saito, A. Osuka, and D. Kim, *J. Am. Chem. Soc.*, 2010, **132**, 3105; f) M. Inoue, T. Yoneda, K. Youfu, N. Aratani, and A. Osuka, *Chem. Eur. J.*, 2011, **17**, 9028.
  - J.-Y. Shin, H. Furuta, K. Yoza, S. Igarashi, and A. Osuka, *J. Am. Chem. Soc.*, 2001, **123**, 7190.
  - a) J. S. Lindsey, I. C. Schreiman, H. C. Hsu, P. C. Kearney, and A. M. Marguerettaz, *J. Org. Chem.*, 1987, **52**, 827; b) R. W. Wagner, D. S. Lawrence, and J. S. Lindsey, *Tetrahedron Lett.*, 1987, **28**, 3069.

10. a) R. Taniguchi, S. Shimizu, M. Suzuki, J.-Y. Shin, H. Furuta, and A. Osuka, *Tetrahedron Lett.*, 2003, **44**, 2505; b) Y. Kamimura, S. Shimizu, and A. Osuka, *Chem. Eur. J.*, 2007, **13**, 1620; c) Y. Tanaka, J.-Y. Shin, and A. Osuka, *Eur. J. Org. Chem.*, 2008, 1341.
11. M. Suzuki and A. Osuka, *Org. Lett.*, 2003, **5**, 3943.
12. B. Frank and A. Nonn, *Angew. Chem. Int. Ed. Engl.*, 1995, **34**, 1795.
13. a) P. J. Brothers, *J. Porphyrins Phthalocyanines*, 2002, **6**, 259; b) P. J. Brothers, *Chem. Commun.*, 2008, 2090.
14. T. Köhler, M. C. Hodgson, D. Seidel, J. M. Veauthier, S. Meyer, V. Lynch, P. D. W. Boyd, P. J. Brothers, and J. L. Sessler, *Chem. Commun.*, 2004, 1060.
15. C. J. Carrano and M. Tsutsui, *J. Coord. Chem.*, 1977, **7**, 125.
16. W. J. Belcher, P. D. W. Boyd, P. J. Brothers, M. J. Liddell, and C. E. F. Rickard, *J. Am. Chem. Soc.*, 1994, **116**, 8416.
17. W. J. Belcher, M. Breede, P. J. Brothers, and C. E. F. Rickard, *Angew. Chem. Int. Ed.*, 1998, **37**, 1112.
18. a) A. Weiss, H. Pritzkow, P. J. Brothers, and W. Siebert, *Angew. Chem. Int. Ed.*, 2001, **40**, 4182; b) A. Weiss, M. C. Hodgson, P. D. W. Boyd, W. Siebert, and P. J. Brothers, *Chem. Eur. J.*, 2007, **13**, 5982.
19. A. Młodzianowska, L. Latos-Grażyński, L. Szterenberga, and M. Stępień, *Inorg. Chem.*, 2007, **46**, 6950.
20. J. K. Sanders, N. Bampos, Z. Clyde-Watson, S. L. Darling, J. C. Hawley, H.-J. Kim, C. C. Mak, and S. J. Webb, 'The Porphyrin Handbook: Axial Coordination Chemistry of Metalloporphyrins,' Vol. 3, ed. by K. M. Kadish, K. M. Smith, and R. Guilard, Academic Press, San Diego, 2000, pp. 1–48.
21. P. Sayer, M. Gouterman, and C. R. Connell, *J. Am. Chem. Soc.*, 1977, **99**, 1082.
22. T. Barbour, W. J. Belcher, P. J. Brothers, C. E. F. Rickard, and D. C. Ware, *Inorg. Chem.*, 1992, **31**, 746.
23. Y. Yamamoto, R. Nadano, M. Itagaki, and K. Akiba, *J. Am. Chem. Soc.*, 1995, **117**, 8287.
24. H. Segawa, K. Kunimoto, K. Susumu, M. Taniguchi, and T. Shimizu, *J. Am. Chem. Soc.*, 1994, **116**, 11193.
25. D. R. Reddy and B. G. Maiya, *Chem. Commun.*, 2001, 117.
26. J. Li, L. R. Subramanian, and M. Hanack, *Eur. J. Org. Chem.*, 1998, 2759.
27. B. Ramdhanie, C. L. Stern, and D. P. Goldberg, *J. Am. Chem. Soc.*, 2001, **123**, 9447.
28. A. Młodzianowska, L. Latos-Grażyński, and L. Szterenberga, *Inorg. Chem.*, 2008, **47**, 6364.
29. E. Pacholska-Dudziak, F. Ulatowski, Z. Ciunik, and L. Latos-Grażyński, *Chem. Eur. J.*, 2009, **15**, 10924.

30. Y. Matano and H. Imahori, *Acc. Chem. Res.*, 2009, **42**, 1193.
31. K. Moriya, S. Saito, and A. Osuka, *Angew. Chem. Int. Ed.*, 2010, **49**, 4297.
32. S. Saito and A. Osuka, *Chem. Eur. J.*, 2006, **12**, 9095.
33. C. G. Claessens, D. González-Rodríguez, and T. Torres, *Chem. Rev.*, 2002, **102**, 835.
34. a) Y. Inokuma and A. Osuka, *Dalton. Trans.*, 2008, 2517; b) A. Osuka, E. Tsurumaki, and T. Tanaka, *Bull. Chem. Soc. Jpn.*, 2011, **84**, 679.
35. S. Saito, K. S. Kim, Z. S. Yoon, G. Kim, and A. Osuka, *Angew. Chem. Int. Ed.*, 2007, **46**, 5591.
36. R. Sakamoto, S. Saito, S. Shimizu, Y. Inokuma, N. Aratani, and A. Osuka, *Chem. Lett.*, 2010, **39**, 439.
37. H. Rexhausen and A. Gossauer, *J. Chem. Soc., Chem. Commun.*, 1983, 275.
38. a) J.-Y. Shin, H. Furuta, and A. Osuka, *Angew. Chem. Int. Ed.*, 2001, **40**, 619; b) S. Mori, J.-Y. Shin, S. Shimizu, F. Ishikawa, H. Furuta, and A. Osuka, *Chem. Eur. J.*, 2005, **11**, 2417.
39. T. Yoneda, H. Mori, B. S. Lee, M.-C. Yoon, D. Kim, and A. Osuka, *Chem. Commun.*, 2012, **48**, 6785.
40. T. Higashino and A. Osuka, *Chem. Sci.*, 2012, **3**, 103.
41. M. G. P. M. S. Neves, R. M. Martins, A. C. Tomé, A. J. D. Silvestre, A. M. S. Silva, V. Félix, M. G. B. Drew, and J. A. S. Cavaleiro, *Chem. Commun.*, 1999, 385.
42. a) M. Suzuki and A. Osuka, *Chem. Eur. J.*, 2007, **13**, 196; b) T. Koide, G. Kashiwazaki, M. Suzuki, K. Fukawa, M.-C. Yoon, S. Cho, D. Kim, and A. Osuka, *Angew. Chem. Int. Ed.*, 2008, **47**, 9661.
43. a) S. Shimizu, J.-Y. Shin, H. Furuta, R. Ismael, and A. Osuka, *Angew. Chem. Int. Ed.*, 2003, **42**, 78; b) S. Shimizu, N. Aratani, and A. Osuka, *Chem. Eur. J.*, 2006, **12**, 4909; c) T. Koide, K. Youfu, S. Saito, and A. Osuka, *Chem. Commun.*, 2009, 6047.
44. Y.-S. Xie, K. Yamaguchi, M. Toganoh, H. Uno, M. Suzuki, S. Mori, S. Saito, A. Osuka, and H. Furuta, *Angew. Chem. Int. Ed.*, 2009, **48**, 5496.
45. J. Sankar, S. Mori, S. Saito, H. Rath, M. Suzuki, Y. Inokuma, H. Shinokubo, K. S. Kim, Z. S. Yoon, J.-Y. Shin, J. M. Lim, Y. Matsuzaki, O. Matsushita, A. Muranaka, N. Kobayashi, D. Kim, and A. Osuka, *J. Am. Chem. Soc.*, 2008, **130**, 13568.
46. T. Higashino, J. M. Lim, T. Miura, S. Saito, J.-Y. Shin, D. Kim, and A. Osuka, *Angew. Chem. Int. Ed.*, 2010, **49**, 4950.
47. S. Saito, J.-Y. Shin, J. M. Lim, K. S. Kim, D. Kim, and A. Osuka, *Angew. Chem. Int. Ed.*, 2008, **47**, 9657.
48. T. Higashino, B. S. Lee, J. M. Lim, D. Kim, and A. Osuka, *Angew. Chem. Int. Ed.*, doi:10.1002/anie.201208147.
49. D. B. Chesnut and L. D. Quin, *Tetrahedron*, 2005, **61**, 12343.

50. T. Miura, T. Higashino, S. Saito, and A. Osuka, *Chem. Eur. J.*, 2010, **16**, 55.

---



**Atsuhiko Osuka** (1954, Aichi) received a PhD from Kyoto University in 1982. In 1979, he started his academic career at Ehime University as an Assistant Professor. In 1984, he moved to Kyoto University, where he became a Professor in 1996. He received the Japanese Photochemistry Award in 1999 and the Chemical Society of Japan Award in 2010. His research interests cover many aspects of synthetic approaches toward novel porphyrin-related compounds with intriguing structures, properties, and functions.

**Tomohiro Higashino** (1986, Osaka) is a PhD student in Osuka's laboratory and is now exploring novel expanded porphyrins by incorporating phosphorus and silicon atoms.